NANO LETTERS

Letter

pubs.acs.org/NanoLett

Lithium-Ion Battery Cycling for Magnetism Control

Qingyun Zhang,[†] Xi Luo,[†] Luning Wang,[‡] Lifang Zhang,[‡] Bilal Khalid,[†] Jianghong Gong,[†] and Hui Wu*[,†]

[†]State Key Laboratory of New Ceramics and Fine Processing, School of Materials Science and Engineering, Tsinghua University, Beijing, 100084, China

[‡]School of Materials Science and Engineering, University of Science and Technology Beijing, Beijing, 100083, China

Supporting Information

ABSTRACT: Magnetization and electric-field coupling is fundamentally interesting and important. Specifically, current- or voltage-driven magnetization switching at room temperature is highly desirable from scientific and technological viewpoints. Herein, we demonstrate that magnetization can be controlled via the discharge−charge cycling of a lithium-ion battery (LIB) with rationally designed electrode nanomaterials. Reversible manipulation of magnetism over 3 orders of magnitude was achieved by controlling the lithiation/delithiation of a nanoscale α-Fe_2O_3-based electrode. The process was completed rapidly under room-temperature conditions. Our results indicate that in addition to energy storage LIBs, which have been under continuous development for several decades, provide exciting opportunities for the multireversible magnetization of magnetic fields.

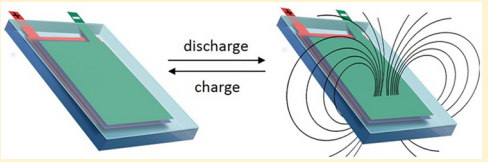

KEYWORDS: *LIB, magnetization control, nano Fe_2O_3, voltage tuning*

The manipulation of magnetism through electric current/voltage actuation has been studied in depth for numerous applications, including spin-electronic devices,[1] giant magnetoresistance and tunnel magnetoresistance sensors,[2] magnetic tunnel junctions (MTJs),[3,4] domain walls (DWs),[5,6] and three-terminal devices that utilize spin−orbit torques.[7,8] In contrast to the magnetization switching approach, which uses electric current and suffers drawback of high energy consumption, electrode-field-control (*E*-control) of magnetization is a promising route because of its expected ultralow power consumption. Recently, this topic has attracted significant attention and researchers have focused on its salient power- and energy-saving features. The electrical control of magnetism is one of the core issues in magnetic phase modification,[9] interfacial magnetization anisotropy,[10,11] coercivity H_C,[12,13] Curie temperature T_C based on carrier concentration,[14] as well as other magnetic properties of numerous material systems. Electric-field magnetization control was first demonstrated in the magnetic semiconductor (In, Mn)As in which a magnetic phase transition and T_C were induced.[9,15] Subsequently, interfacial magnetic anisotropy toggling and coercivity reduction via application of an electric field were observed in a Co/metal-oxide bilayer[16] and the ferromagnetic metal CoFeB,[13] respectively. Thus far, experimental approaches that use electric current/field actuation in semiconductors, ferromagnetic metals, multiferroic materials, and insulator/magnetic metal materials have been integrated into the fields of study of both magnetic and electric devices. While successful, the saturation magnetization M_S or Hall resistance R_H variation range based on the *E*-control of magnetism has thus far been confined to approximately 1 order of magnitude.[17] The voltage-induced modification of magnetism is, in general, limited by the T_C (≪room temperature).[9,18] Specifically, the voltage-induced magnetization of magnetic semiconductors and multiferroics at room temperature is difficult to overcome. Furthermore, the operating conditions and the thermal stability[19] of the device regarding the induced electric field should be investigated further. Therefore, conveniently manipulating magnetization using an electric field remains a challenge, especially in the case of quantitative control and switching of magnetization using voltage changes at room temperature.

Electrochemical energy storage devices, especially LIBs, have experienced rapid development over the past few decades. In principle, lithium atoms are inserted into and extracted from the electrode materials during battery cycling. This electrochemical reaction, which is driven by the current flow of the battery, provides new insights for manipulating the properties of the electrode materials. Specifically, changes in the magnetic properties of many materials are associated with lithium-ion insertion and extraction. Precise adjustment of discharge−charge voltage is typically achieved in a rechargeable LIB. The rechargeable LIB is one of the great successes of modern materials electrochemistry[20] and is undergoing a rapid expansion in portable electronic devices.

Early studies on LIBs focused on lithium intercalation in layered dichalcogenides such as TaS_2,[21] TiS_2,[21] and MoS_2;[22] these LIBs exhibited similar single-phase behaviors upon lithium intercalation. However, in 1991 Sony introduced a metal-oxide-based C/$LiCoO_2$ rocking-chair cell for LIBs to enhance their cycling performance as well as their safety.[23] The successful commercial application of $LiCoO_2$ encouraged subsequent investigations into other metal oxides. Thus, researchers investigated nanostructured electrodes based on

Received: October 21, 2015
Revised: November 26, 2015
Published: December 14, 2015

DOI: 10.1021/acs.nanolett.5b04276
Nano Lett. 2016, 16, 583−587

3d-transition-metal layered oxides referred to as "conversion materials". These materials included Co-, Mn-, Cu-, Ni-, Mo-, W- and Fe-based metal oxides. The most interesting aspects of these new materials were an enlarged effective surface area and an excellent ability to reversibly lithiate/delithiate. In particular, the MoO_3, Co_3O_4, and Fe_3O_4 supported lithiation/delithiation in excess of six lithium atoms per formula unit.[24−26] This advanced performance was due to the nanoscale transition-metal oxides breaking into metal clusters and reacting with lithium to form a LiO_2 matrix, this process was highly reversible.[27]

By considering all important factors for enhancing performance and cycling life of LIBs, we selected alpha-Fe_2O_3 (α-Fe_2O_3) as the electrode material in this work because of its high natural abundance, low cost, and good environmental compatibility.[28] The nanoscal α-Fe_2O_3 particles underwent reversible insertion of six lithium atoms per Fe_2O_3, which was possible because the intercalation/deintercalation of Li^+ into/from Fe_2O_3 is a single-phase process. By contrast, large particles (larger than 1 μm) underwent an irreversible phase transformation when 0.5 lithium atoms per formula unit were extracted.[29] Our intercalation/deintercalation experiments demonstrated for the first time control of magnetic properties via control of the applied voltages during Li^+-ion flow through the α-Fe_2O_3-based electrode. Li^+-ion insertion and extraction into/from the surface of electrodes are possibly the key to converting Fe_2O_3 into Fe via the following chemical reaction:[30]

$$Fe_2O_3 + 6Li^+ + 6e^- \Leftrightarrow 3Li_2O + 2Fe \quad (1)$$

This reversible chemical reaction led to our observation of an interesting phenomenon (Figure 1b,c). Specifically, magnetization/demagnetization cycles coincided with the repeatition of the lithiation/delithiation process. Furthermore, magnetization manipulation of the LIB at room temperature coincidently combines the fields of electrochemistry and magnetism. Additionally, Li^+-ion flow resembles a rocking-chair motion between two electrodes and bridges the fields of electrochemistry and magnetism.

We designed a simple punched cell to demonstrate magnetization control in a LIB. Figure 1a is a schematic of the predesigned experimental device, which comprises an anode, a cathode, a separator, and electrolyte (Supporting Information Figure S1). These materials were sealed with the plastic film (Polyethylene terephthalate, PET) using a plastic-envelop machine in an argon-filled glovebox. The assembled LIB (Figure 1a) was subsequently used as an experimental device to demonstrate manipulation magnetization.

LIBs typically require long discharge−charge cycle time, particularly during the initial discharge−charge process. Thus, by referring to the first discharge−charge curve (Figure 2a and Supporting Information Figure S2a), we selected 10 voltage points during the first discharge−charge process to observe magnetization changes of the experimental device resulting from changes in the discharge−charge state. For the first lithiation (first discharge) process, we used vibrating sample magnetometry (VSM) to investigate magnetization changes of the device at room temperature. Taking the first discharge voltage curve into account, we examined the effect of the discharge-potential-induced lithiation state on the magnetic properties of the device. The magnetic properties were characterized at five discharge voltage points recorded in Figure 2a. As the discharge potential gradually decreased, a remarkable change in the hysteresis loops was observed, along

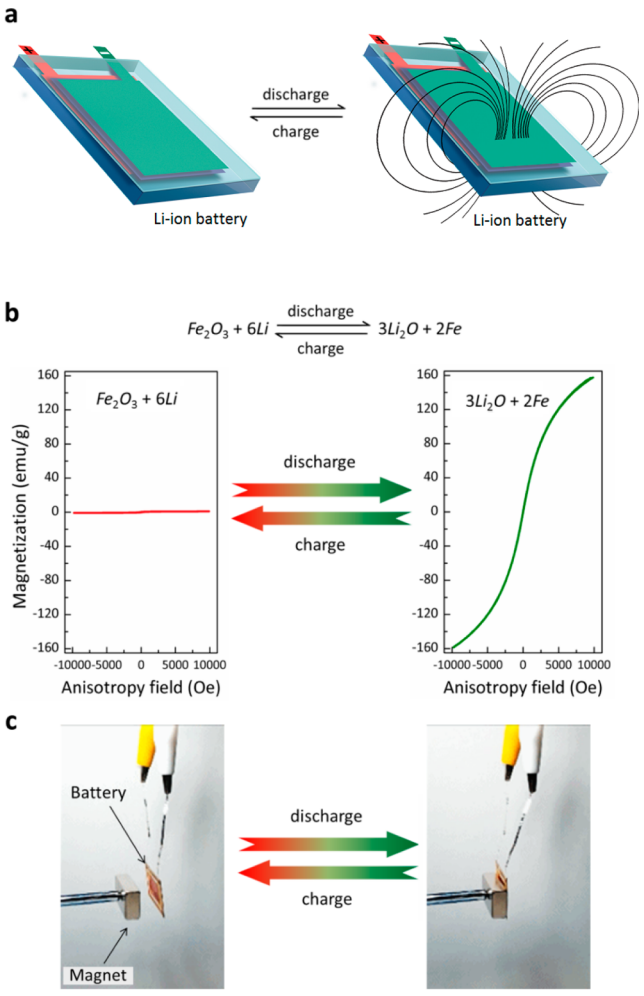

Figure 1. (a) Schematic of the predesigned pouch cell used as the experimental device. (b) Illustration of the relationship between magnetization control and the lithiation/delithiation reaction in the lithium-ion battery (Li/α-Fe_2O_3). (c) A true representation of the phenomenon of reversible magnetization control through voltage tuning.

with an increase in the M_S value (Figure 2b). This behavior was attributed to the Fe_2O_3 to Fe conversion that accompanied the enhanced lithiation state. Thus, the predesigned device was reasonably assumed to have been magnetized through the lithiation process.

With the aim of reversibly manipulating the magnetization of the experimental device, we demonstrated that the magnetized device could be demagnetized via the delithiation process. Subsequently, we also selected five points of charge potential recorded in Figure 2a and performed VSM measurements on the magnetized device during the first delithiation process (first charge). As shown in Figure 2c, with increasing charge potential the hysteresis loop exhibited a decrease in M_S, which is explained by the decrease in Fe content as consequence of the delithiation process. Similarly, demagnetization of the experimental device was achieved via the delithiation process. During the lithiation/delithiation process, we observed a reversible magnetization/demagnetization processes in the experimental device at room temperature.

Considering a significant magnetization variation of the experimental device, Figure 2d summarizes the results for the M_S and H_C changes during the first lithiation and delithiation

DOI: 10.1021/acs.nanolett.5b04276
Nano Lett. 2016, 16, 583−587

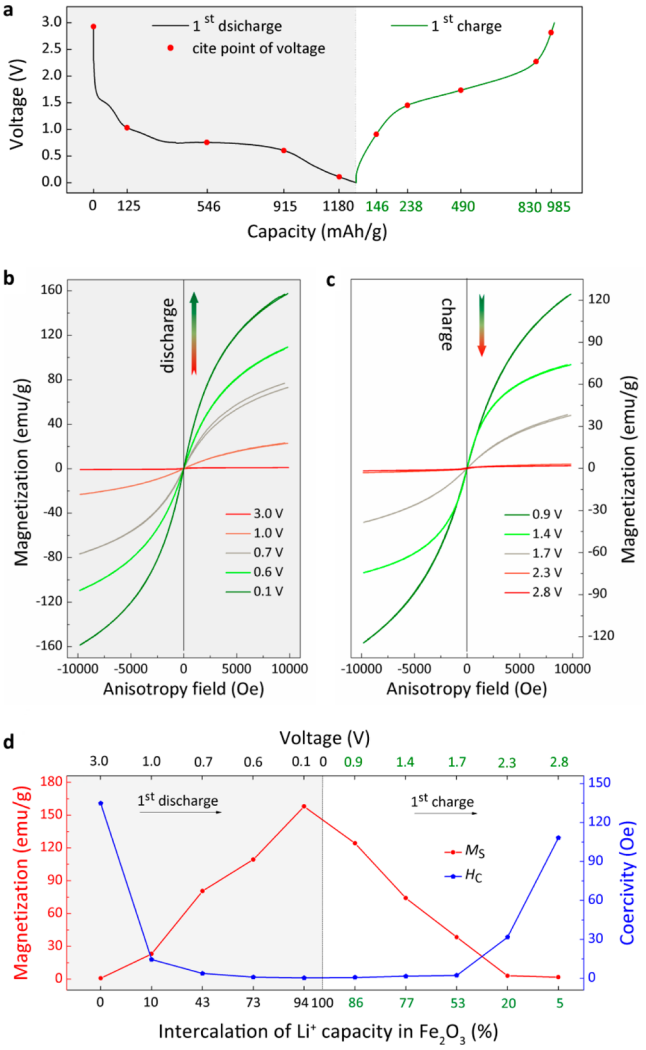

Figure 2. (a) The initial discharge−charge curve recorded at the indicated voltage points for manipulating magnetization during the first lithiation/delithiation process. (b,c) Magnetic hysteresis loops of the experimental device that was discharged and charged at different voltages during the first discharge−charge process. (d) Change of magnetization saturation and coercivity of the experimental device at different discharge−charge voltages during the first lithiation/delithiation process.

process at room temperature. During the first discharge process, the M_S value varied from 0.90 to 158.039 emu/g, whereas the H_C value decreased from 134.85 to 0.436 Oe during the discharge process. Both the M_S and H_C values exhibited substantial changes, varying by 3 orders of magnitude; this variation is an excellent result compared with that achieved via magnetization manipulation based on current or *E* actuation.[13,31] These magnetization changes are attributed to an intrinsic conversion reaction between Fe_2O_3 and Fe in the electrode of the experimental device. The magnetization switching mechanism is based on lithiation/delithiation and is described as an electrochemical reaction,[30] as previously mentioned. In the aforementioned reaction, $LiFeO_2$ is one of the main phases formed during the lithiation process. Nevertheless, the new crystalline phases produced via the lithiation/delithiation reaction are relatively complex. The specific phases responsible for the remarkable changes on the M_S and H_C of the experimental device need to be determined.

To further characterize the phase changes that occurred during the magnetization/demagnetization processes, we performed powder X-ray diffraction (XRD) measurements on the cathode material of the device at five similar voltage points during the first discharge process. Figure 3 depicts the XRD

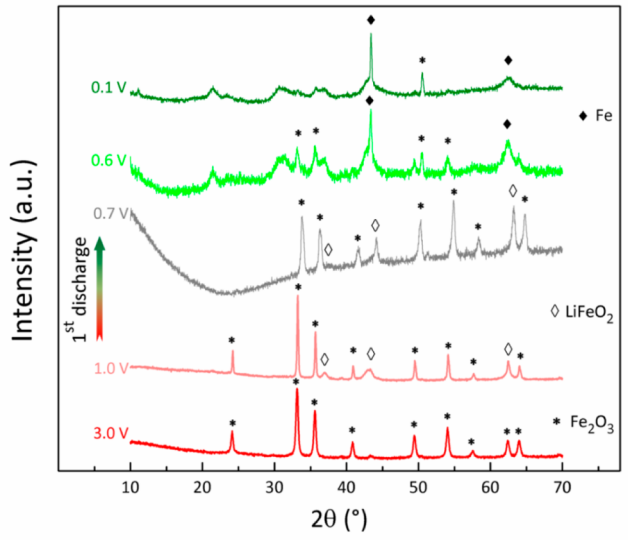

Figure 3. X-ray diffraction patterns of the experimental device during the first lithiation reaction at five selected discharge voltages.

patterns of a pristine electrode (at the beginning of the first discharge, 3.0 V) and a lithiated Fe_2O_3-based electrode after galvanostatic discharge at 200 mA/g in the voltage range from 1.0 to 0.1 V. As evident in Figure 3, new phases appeared at 1.0, 0.7, 0.6, and 0.1 V, and the Fe_2O_3 phase began to gradually disappear at 1.0 V. Meanwhile, the peaks associated with lithium iron oxide ($LiFeO_2$) phases in the XRD patterns of the lithiated electrodes recorded for the discharge voltage range from 1.0 to 0.7 V increased in intensity; the patterns typically contained peaks centered at 2θ values of 37.5, 43.4, and 63.1°.[29] An increase in the amount of $LiFeO_2$ formed implies that more lithium intercalated into Fe_2O_3, resulting in an increase in the overall amount of the iron phases. This increase in the amounts of iron phases closely coincides with the observation that the single-phase insertion of Li and the reduction of Fe^{3+} in Fe_2O_3 occurred at approximately 0.71 V (Supporting Information Figure S5). Starting at 0.6 V, the δ-Fe phase with typical peaks at 43.6° and 63.4° was identified. The presence of Fe suggests the formation of other lithium oxides,[32] which appear to be amorphous (XRD patterns at 0.6 and 0.1 V in Figure 3) and are therefore not readily detected by XRD. Furthermore, in comparison with the XRD pattern of crystalline hematite (α-Fe_2O_3) at the first discharge potential of 3.0 V, the XRD pattern of the material at a discharge potential of 0.1 V changed significantly and the major crystal phase of iron and several amorphous lithium oxide phase were observed. Therefore, the active electrode material Fe_2O_3 is reasonably assumed to undergo a conversion reaction of $Fe_2O_3 \rightarrow LiFeO_2 \rightarrow Fe$ after the first discharge process. Thus, the experimental device exhibits a remarkable magnetization change from weak to strong that correlates with a decrease in the discharge voltage. This change is in good agreement with previous results (Figure 2d), whereby an increase in M_S and a decrease in H_C were

DOI: 10.1021/acs.nanolett.5b04276
Nano Lett. 2016, 16, 583−587

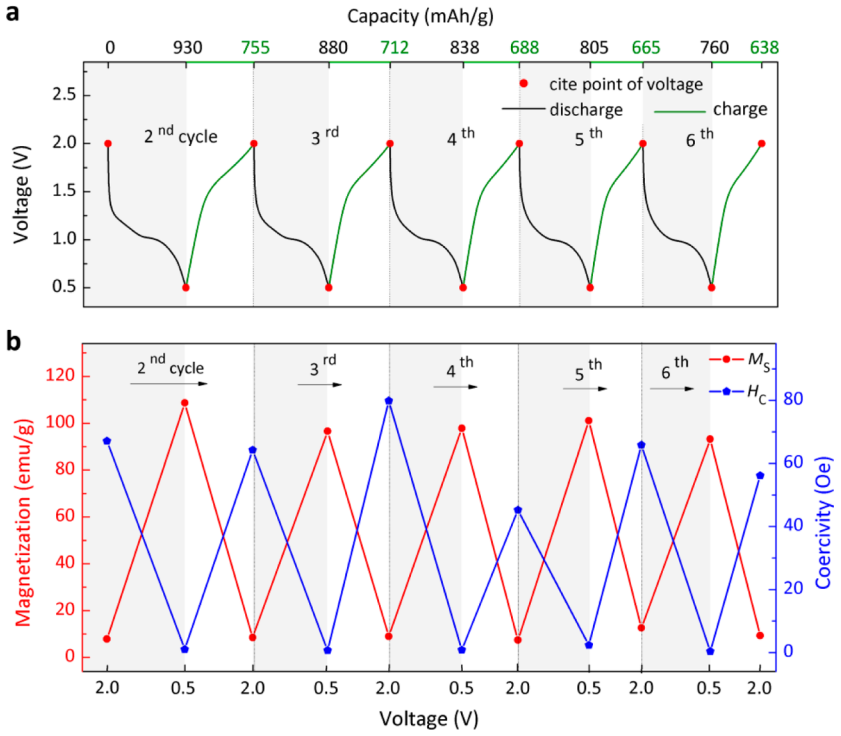

Figure 4. (a) The discharge−charge curves ranging from the second to the sixth cycle; the curves are shown for the selected voltage points for manipulating magnetization during five consecutive lithiation/delithiation processes. (b) Change of the saturation magnetization and coercivity of the experimental device at different discharge−charge voltages during the second to the sixth lithiation/delithiation processes.

observed with decreasing voltage during the first discharge process.

As previously discussed, reversible magnetization manipulation was achieved through the voltage-tuning lithiation/delithiation state in a LIB during the first discharge−charge process. Nevertheless, from technological and commercial viewpoints a repeatedly reversible or multireversible technology for manipulating magnetization may represent an innovative technology that is useful in products. To determine whether the magnetization/demagnetization processes remained reversible after the experimental device was subjected to several discharge−charge cycles, we performed a similar magnetization test on the experimental device after multiple discharge−charge cycles. As indicated in Figure 4a, beginning from the second discharge−charge cycle, we performed five discharge−charge cycles at room temperature in the voltage window from 2.0 to 0.5 V. The voltage points at 2.0 and 0.5 V during each cycle were selected for observation of changes in the magnetic properties of the device.

Figure 4b depicts the M_S and H_C changes in detail. We observed that the M_S value fluctuated between ca. 10 and 100 emu/g following the lithiation/delithiation processes that occurred during cycling between 0.5 and 2.0 V. The H_C ranged between ca. 1 and 80 Oe. In addition, M_S increased while H_C decreased during each lithiation process, and M_S decreased while H_C increased during each delithiation process. These results are similar to those observed for the first lithiation and delithiation processes (Figure 2d). Consequently, the reversible magnetization and demagnetization via the lithiation/delithiation reaction for five discharge−charge cycles approximates a switching effect. Furthermore, these results confirm that similar processes can be controlled during each discharge−charge cycle, which represents a multireversible manipulation of magnetization based on the voltage-tuning lithiation/delithiation state.

In conclusion, the multireversible magnetization of ferromagnetic material can be controlled via the lithiation/delithiation reaction in a LIB by varying the discharge−charge potential at room temperature. This phenomenon couples two important fields, magnetism and electrochemistry, and enables precise quantitative magnetization manipulation using an electrochemical method. Magnetization control using the voltage-tuning lithiation/delithiation state approach is based on an electrochemical mechanism and will be applicable to the majority of modern α-Fe_2O_3-type magnetic materials. Our work reveals that magnetic properties are linked to the voltage control of LIBs. The concept of tuning physical properties using battery cycling clearly has strong potential because hundreds of active materials have already been developed as LIB electrodes.

■ ASSOCIATED CONTENT

Supporting Information

The Supporting Information is available free of charge on the ACS Publications website at DOI: 10.1021/acs.nanolett.5b04276.

Details of sample preparation, data acquisition, and the data analysis. (PDF)

Video demonstrating the magnetization change during the first discharge-charge process. (AVI)

■ AUTHOR INFORMATION

Corresponding Author

*E-mail: huiwu@tsinghua.edu.cn.

Author Contributions

Q.Z. and X.L. contributed equally.

DOI: 10.1021/acs.nanolett.5b04276
Nano Lett. 2016, 16, 583−587

Notes

The authors declare no competing financial interest.

■ ACKNOWLEDGMENTS

This study was supported by the National Basic Research of China (Grants 2015CB932500 and 2013CB632702) and the NSF of China (Grants 51522207 and 51302141).

■ REFERENCES

(1) Slonczewski, J. C. *J. Magn. Magn. Mater.* **1996**, *159*, L1−L7.
(2) Weisheit, M.; Fähler, S.; Marty, A.; Souche, Y.; Poinsignon, C.; Givord, D. *Science* **2007**, *315*, 349−351.
(3) Mangin, S.; Ravelosona, D.; Katine, J. A.; Carey, M. J.; Terris, B. D.; Fullerton, E. E. *Nat. Mater.* **2006**, *5*, 210−215.
(4) Ikeda, S.; et al. *SPIN* **2012**, *2*, 1240003−1240015.
(5) Khvalkovskiy, A. V.; Apalkov, D.; Watts, S.; Chepulskii, R.; Beach, R. S.; Ong, A.; Krounbi, M. *J. Phys. D: Appl. Phys.* **2013**, *46*, 074001−74020.
(6) Catalan, G.; Seidel, J.; Ramesh, R.; Scott, J. F. *Rev. Mod. Phys.* **2012**, *84*, 119−156.
(7) Chernyshov, A.; Overby, M.; Liu, X.; Furdyna, J. K.; Lyanda-Geller, Y.; Rokhinson, L. P. *Nat. Phys.* **2009**, *5*, 656−659.
(8) Liu, L.; Pai, C. F.; Li, Y.; Tseng, H. W.; Ralph, D. C.; Buhrman, R. A. *Science* **2012**, *336*, 555−558.
(9) Ohno, H.; Chiba, D.; Matsukura, F.; Omiya, T.; Abe, E.; Dietl, T.; Ohtani, K. *Nature* **2000**, *408*, 944−946.
(10) Maruyama, T.; Shiota, Y.; Nozaki, T.; Ohta, K.; Toda, N.; Mizuguchi, M.; Suzuki, Y. *Nat. Nanotechnol.* **2009**, *4*, 158−161.
(11) Nakamura, K.; Shimabukuro, R.; Fujiwara, Y.; Akiyama, T.; Ito, T.; Freeman, A. *Phys. Rev. Lett.* **2009**, *102*, 187201−187205.
(12) Yamanouchi, M.; Chiba, D.; Matsukura, F.; Ohno, H. *J. Appl. Phys.* **2006**, *45*, 3854.
(13) Sawicki, M.; Chiba, D.; Korbecka, A.; Nishitani, Y.; Majewski, J. A.; Matsukura, F.; Ohno, H. *Nat. Phys.* **2010**, *6*, 22−25.
(14) Dietl, T.; Ohno, H.; Matsukura, F. *Phys. Rev. B: Condens. Matter Mater. Phys.* **2001**, *63*, 195205−195226.
(15) Bauer, U.; Yao, L.; Tan, A. J.; Agrawal, P.; Emori, S.; Tuller, H. L.; Beach, G. S. *Nat. Mater.* **2014**, *14*, 174−181.
(16) Wang, W. G.; Li, M.; Hageman, S.; Chien, C. L. *Nat. Mater.* **2012**, *11*, 64−68.
(17) Matsukura, F.; Tokura, Y.; Ohno, H. *Nat. Nanotechnol.* **2015**, *10*, 209−220.
(18) Chiba, D.; Fukami, S.; Shimamura, K.; Ishiwata, N.; Kobayashi, K.; Ono, T. *Nat. Mater.* **2011**, *10*, 853−856.
(19) Awschalom, D. D.; Flatté, M. M. *Nat. Phys.* **2007**, *3*, 153−159.
(20) Tarascon, J. M.; Armand, M. *Nature* **2001**, *414*, 359−367.
(21) Gamble, F. R.; Osiecki, J. H.; Cais, M.; Pisharody, R.; DiSalvo, F. J.; Geballe, T. H. *Science* **1971**, *174*, 493−497.
(22) Haering, R. R. Stiles, J. A. R. Brandt, K. U.S. Patent 4,224,390, 1980.
(23) Mohri, M.; Yanagisawa, N.; Tajima, Y.; Tanaka, H.; Mitate, T.; Nakajima, S.; Wada, H. *J. Power Sources* **1989**, *26*, 545−551.
(24) Du, N.; Zhang, H.; Chen, B. D.; Wu, J. B.; Ma, X. Y.; Liu, Z. H.; Tu, J. P. *Adv. Mater.* **2007**, *19*, 4505−4509.
(25) Taberna, P. L.; Mitra, S.; Poizot, P.; Simon, P.; Tarascon, J. M. *Nat. Mater.* **2006**, *5*, 567−573.
(26) Chernova, N. A.; Roppolo, M.; Dillon, A. C.; Whittingham, M. S. *J. Mater. Chem.* **2009**, *19*, 2526−2552.
(27) Poizot, P.; Laruelle, S.; Grugeon, S.; Dupont, L.; Tarascon, J. M. *Nature* **2000**, *407*, 496−499.
(28) Reddy, M. V.; Yu, T.; Sow, C. H.; Shen, Z. X.; Lim, C. T.; Rao, G. S.; Chowdari, B. V. R. *Adv. Funct. Mater.* **2007**, *17*, 2792−2799.
(29) Larcher, D.; Masquelier, C.; Bonnin, D.; Chabre, Y.; Masson, V.; Leriche, J. B.; Tarascon, J. M. *J. Electrochem. Soc.* **2003**, *150*, A133−A139.
(30) Chen, J.; Xu, L.; Li, W.; Gou, X. *Adv. Mater.* **2005**, *17*, 582−586.
(31) Endo, M.; Matsukura, F.; Ohno, H. *Appl. Phys. Lett.* **2010**, *97*, 222501−222504.
(32) Brandt, A.; Winter, F.; Klamor, S.; Berkemeier, F.; Rana, J.; Pöttgen, R.; Balducci, A. *J. Mater. Chem. A* **2013**, *1*, 11229−11236.

DOI: 10.1021/acs.nanolett.5b04276
Nano Lett. 2016, 16, 583−587